

Preparation, physicochemical and stability studies of chitosan-PNIPAM based responsive microgels under various pH and temperature conditions

Abbas Khan^{1,2} · Muhammad Bisyrul H. Othman¹ · Boon Peng Chang¹ · Hazizan Md Akil¹

Received: 2 October 2014 / Accepted: 1 March 2015 / Published online: 10 March 2015
© Iran Polymer and Petrochemical Institute 2015

Abstract This study describes the synthesis, characterization and detailed physicochemical investigation on the stimuli-responsive behaviour of chitosan-poly (*N*-isopropylacrylamide) [chitosan-PNIPAM] copolymer microgels. Six different compositions of dual-responsive chitosan-PNIPAM based microgels were synthesized by soapless-emulsion free radical copolymerization method in an aqueous medium at 70 °C. The chemical composition, swelling/de-swelling, volume phase transitions, electrical properties, colloidal stability, and physicochemical behaviour under various pH/temperature conditions were investigated using Fourier transform infrared spectroscopy (FTIR), dynamic light scattering (DLS), zeta-potential, and rheology. Various functional groups present in the copolymer microgels were confirmed by FTIR analysis. The hydrodynamic diameter (D_h), volume phase transition temperature (VPTT), and swelling/de-swelling behaviour of microgels, under different pH and temperature conditions, in aqueous media were investigated using DLS measurements. Zeta potential measurements were used to evaluate the stability, electrical and electro-kinetic properties of the gels at various pH/temperatures. Likewise, the influence of temperature and chemical composition of microgels on the particle behaviour was investigated through rheological studies.

A transition from sol-to-gel state at temperature beyond 50 °C was also noticed in all hydrogel samples. On the basis of results obtained, we observed that variables such as NIPAM/chitosan ratio, amount of cross-linker, and temperature/pH not only affect the above mentioned properties but also affect the dual-sensitivity and stability of the microgels. Most of the chitosan-PNIPAM particles remained soluble and maintained good stability without significant sedimentation in water through a wide range of pH (pH \approx 2–8) for about 3 months at room temperature.

Keywords Light scattering · Stimuli-responsive polymers · Phase changes · Physicochemical properties · Colloidal stability

Introduction

Due to their tunable dimensions, large surface areas, stable interior network structure, and a very short response time, polymer macro/micro/nano and hydrogels are playing an important part in a diverse range of applications. Polymer microgels have rapidly gained importance in the field of materials science owing to their potential applications in biomedical [1], pollution control [2] enhanced oil recovery [3], sensors [4], controlled release of encapsulated drugs in response to environmental changes [5], the fabrication of photonic crystals, glucose sensing [6] template-based synthesis of inorganic nanoparticles [7] and chemical separation [8]. These numerous applications of microgels arise from their ability to undergo reversible volume phase transitions in response to external stimuli such as a change in pH [9], temperature [10] and ionic strength of the surrounding medium [11].

✉ Abbas Khan
abbas053@gmail.com

✉ Hazizan Md Akil
Hazizan@eng.usm.my

¹ School of Materials and Mineral Resources Engineering, Engineering Campus, Universiti Sains Malaysia, 14300 Nibong Tebal, Pulau Pinang, Malaysia

² Department of Chemistry, Abdul Wali Khan University Mardan, Mardan 23200, Pakistan

To prepare stimuli-responsive hydrogels for biomedical applications, natural biopolymers have been considered as suitable candidates due to their biocompatibility, low toxicity, excellent biodegradability, and high content of functional groups [12–14]. Because of the unusual properties of various biopolymers, such as chitosan, they are considered to be versatile materials, with extensive applications in biomedical, biotechnological, and nano-biotechnological fields [15, 16]. Of the commonly available biopolymers, natural polysaccharides, such as alginate, hyaluronic acid, dextran, and chitosan, have been proposed for biomedical purposes, due to their biodegradability and biocompatibility [17–19]. Among the known polysaccharides, chitosan is quite unique, not only due to its antibacterial, biodegradable, biocompatible and mucoadhesive properties but also because of its glucosamine groups, cationicity, and capacity to form polyelectrolyte complexes [20]. However, chitosan is originally insoluble in some solvents and brittle in nature, which limits its potential industrial applications, as compared to other synthetically available polymers. To obtain desirable properties, modification of chitosan by chemical/physical methods and compounding it with other moieties, are of prime importance. In connection to this, Zhang et al. [21] have reported the rational design of pH-responsive chitosan-based microgels for biomedical applications for the first time.

Further, to explore the applications and understand the fundamental mechanism of stimuli-responsive behaviour of chitosan-based microgels, it is important to undertake the detailed physicochemical studies of these hydrogels in aqueous media. It is known to us that most of the studies related to chitosan-based hydrogels have focused on the applied side while the basic physicochemical investigations of these hydrogels have been less addressed. Importantly, physicochemical properties not only affect the absorption and release processes of drugs, but also govern the interaction of particles with different biological compounds (i.e. proteins or membranes) of the tissue where they are introduced. Thus, successful development of polymeric particles to act as drug delivery vehicles can easily be determined by a detailed knowledge of their chemical nature and physical properties, which would explain how they interact with their potential biological environment/system [22]. Numerous workers have reported the physicochemical characterization of chitosan homogels, but they have specifically focused on macroscopic films [23, 24], microspheres obtained by covalent cross-linking [25, 26], and nanoparticles achieved by the direct precipitation of chitosan chains without cross-linking agents [27]. Therefore, this lack of information on the fundamental physicochemical studies of chitosan-based responsive copolymer gel/hydrogels needs to be addressed. To better understand the fundamentals and explore new-fangled methods in the field of chitosan-based

responsive copolymer gels; one has to know in detailed manner, the effect of various internal and external parameters on their physicochemical properties. Amongst the tuning actors, the chemical nature, feeding composition of reacting species, and the physical state of the resultant gel can be considered as internal parameters. Meanwhile, the nature of solvent, co-solvent, temperature, and pH, and the addition of electrolytes, are categorized as external parameters. Thus, to attain a microgel system with desirable properties, the tuning of both internal as well as external parameters is of the utmost importance.

To increase the application capability of polymer macro/micro/nanogels and hydrogels especially in the fields of biomedical and nano-technology, the adjustment of their temperature and pH-sensitivity is greatly required [21, 28]. It is so because the polymer–polymer and the polymer–solvent interactions can show an unexpected re-adjustment in small ranges of pH or temperature changes, and this is translated into a chain transition between extended and compacted coil states. For the pH-sensitive polymers, the key element of the system is the presence of ionizable weak acidic or basic moieties attached to a hydrophobic backbone. In case of temperature-responding polymers, usually there exists a fine hydrophobic–hydrophilic balance in their structure. Thus, some changes in the solution temperature around the critical temperature make the chains to collapse or to expand responding to the new adjustments of the hydrophobic and hydrophilic interactions between the polymeric chains and the aqueous media [29]. Among the polymers sensitive to temperature changes, poly (*N*-isopropylacrylamide) [PNIPAM] is a widely studied temperature responsive polymer microgel [30]. It is because PNIPAM has a low critical solution temperature (LCST) at around 32 °C in water. The soluble and flexible coil of PNIPAM converts into a compact globular and insoluble state at or above its LCST. Furthermore, the most important thing from physicochemical and application point of view is that these conformational changes from coil to globular form with solution temperature are reversible [31]. Hence, hydrogels composed of PNIPAM experience a reversible volume change at a similar transition temperature in aqueous media. From application point of view, microgels would be much favourable if they could respond to several stimuli simultaneously. Therefore, *N*-isopropylacrylamide (NIPAM) is copolymerized with several ionic/non-ionic monomers to produce multi-responsive microgels [28, 30]. Chitosan-PNIPAM based copolymer hydrogels are expected to have good potential application in biomedical field. Mani et al. [32] have recently reviewed stimuli-responsive microgels based on polysaccharides with PNIPAM as novel biomaterials. To the best of our knowledge, most of the studies on chitosan-PNIPAM based hydrogels have focused on the applied side. Though, insufficient

Table 1 Summary of gel compositions, zeta potential values and hydrodynamic diameter at pH = 6 and $T = 25\text{ }^{\circ}\text{C}$

Gel designation	Composition of gel (mg/100 mL) ^a	Cross-linker MBA (mg/100 mL)	Zeta potential (mV)	D_h (nm) ^b
ACG01	500:500:10	10	0.576	160
ACG02	500:500:20	20	0.082	295
ACG04	500:1000:10	10	0.187	396
ACG05	500:1000:30	30	0.301	396
ACG06	500:1500:20	20	0.188	342
ACG07	500:1000:20	20	0.288	458

^a Composition of gel = Chitosan:NIPAM:MBA

^b Hydrodynamic diameter in the scale of nanometer

studies are available that have addressed the basic physico-chemical investigation and stability of such micro/hydrogels under various environmental stimuli.

Therefore, to highlight, address and further explore the fundamentals of chitosan-PNIPAM based micro/hydrogel system, herein we report the synthesis and detailed physicochemical study of swelling/deswelling patterns, electrical properties, colloidal stability, volume phase changes, and rheological behaviour of chitosan-based responsive [chitosan-poly(*N*-isopropylacrylamide), (chitosan-PNIPAM)] copolymer hydrogels, at different gel compositions, and under various pH/temperatures in water. Moreover, on the basis of experimental results, an attempt has been made to explain the behaviour of these microgels under various solution conditions using proposed theories.

Experimental

Materials

N-Isopropylacrylamide (NIPAM), *N,N*-methylenebisacrylamide (MBA), and chitosan ($M_w \approx 160,000$ g/mol, degree of deacetylation $\approx 91\%$), were purchased from Aldrich, while all other chemicals were obtained from Acros. NIPAM was purified by recrystallization from toluene/*n*-hexane (1:3) mixture, whilst all other chemicals were used as received and without further purification. Deionized distilled water (ddH₂O), used for all reactions, solution preparations, and microgel purifications, and was obtained from a Millipore Milli-Q system (Millipore, Bedford, MA, USA).

Preparation of the microgel

Chitosan-PNIPAM based hydrogel samples were synthesized by free radical surfactant-free emulsion copolymerization of chitosan, NIPAM, and MBA, using APS as an initiator, following the previously reported procedure [33]. However, some desired modifications were made to the earlier synthetic method. The detail of the composition of

microgels and their respective codes are given in Table 1. During the preparation of microgels, approximately 500 mg of chitosan was dissolved with different amounts of NIPAM and acetic acid in 100 mL doubly distilled and deionized water, under constant magnetic stirring, for approximately 18–20 h, in a three-neck round bottom flask, equipped with an N₂ gas inlet and condenser. The purpose of addition of acetic acid (3–4 mL of 0.05 M) to the reaction system was to ionize the –NH₂ groups of the chitosan to form the –NH₃⁺ groups, so that the chitosan may easily dissolve in the aqueous reaction medium, and hence increase its degree of coupling to NIPAM/PNIPAM. After 20 h stirring under N₂ purging at 30 °C, MBA (used as a cross-linker) was added to the reaction flask. The temperature of the reaction mixture was slowly raised to 70 °C by gradual heating in a silicon filled oil bath under N₂ purging with continuous stirring. After 30–40 min of constant heating at 70 °C, 5 mL of APS (0.05 M) was added to the reaction mixture, to start the polymerization reaction. Several minutes after the addition of the initiator, the colour of the reaction mixture turned light milky and then slightly opaque with time during the course of reaction. The polymerization reaction was allowed to proceed for 5 h at constant stirring under N₂ purging at 70 °C. The resultant copolymer microgels were then purified by centrifugation (Thermo Electron Co. SORVALL[®] RC-6 PLUS super-speed centrifuge) and decantation, and then washed with water. Next, the obtained microgel was further purified by dialysis for 1 week (Spectra/Por[®] molecularporous membrane tubing, cut-off 12,000–14,000, the same below was used) against a diluted HCl solution in water, with a pH of $\sim 5 \pm 0.3$ at room temperature ($\sim 25\text{ }^{\circ}\text{C}$). To maintain constant pH (pH ≈ 5) of the dialysis medium and ensure better purification of the microgel, the diluted aqueous solution of HCl was regularly changed throughout purification process.

Characterization

FTIR analysis was carried out to identify various functional groups present in the microgels. A Perkins-Elmer

Spectroscopy was used to record the FTIR spectra of the oven dried microgel samples. All FTIR spectra of the samples were obtained in the range 500–4000 cm^{-1} . The pH values of the hydrogel systems were measured by using a WTW-Inolab-pH-720 pH meter. Zeta potential measurements were performed with the help of a Malvern Zetasizer, NANO ZS (Malvern Instruments Limited, UK), using a He–Ne laser with a wavelength of 633 nm, and a detector angle of 173°. Original microgel samples were diluted in the desired buffer or electrolyte solution, as per the experimental requirement. Data was obtained from the average of six measurements at a stationary level in a cylindrical cell. Standard deviation was always below 5 %.

The rheological behaviour of hydrogels in aqueous solution was investigated by measuring the change in viscosity using a cone and plate viscometry (Physica MCR301 Rheometer, Anton Paar Austria). The rheometer was equipped with Temperature Control-Peltier Systems (−40 to 200 °C). The temperature dependence of shear stress and hence viscosity was noted using parallel plate–plate arrangement measuring system. The distance between the plates was 0.2 mm (PP25-SN24578, $d = 0.2$ mm). The temperature range for experiment was 25–75 °C with a heating rate of 0.033 °C per second and a fixed shear rate of 50/s.

Likewise, dynamic laser light scattering (DLS) measurements for size determination were performed on a standard Malvern Zetasizer, NANO ZS (Malvern Instruments Limited, UK), using a He–Ne laser with a wavelength of 633 nm, and a detector angle of 90°. All microgel solutions were passed through Millipore Millex-HV filters (with a pore size of 0.80 μm) to remove dust before the DLS measurements. All solutions were equilibrated at each chosen temperature/pH for approximately 10–15 min before measurement. Experimental durations were in the range 5–10 min, and each was repeated three or more times. The scattering intensities for each microgel were measured at pH range from 1 to 11 and temperatures (ranging from 20 to 70 °C). The constrained regularized CONTIN method was used to analyze the correlation functions from DLS and to obtain distribution decay rates and hence the hydrodynamic size (D_h) of hydrogels. Further detail of these analysis/results is discussed in the results and discussion section.

Results and discussion

FTIR results

The free radical copolymerization of chitosan, NIPAM and MBA, using APS as an initiator, was used to prepare chitosan-PNIPAM based microgels by employing soapless

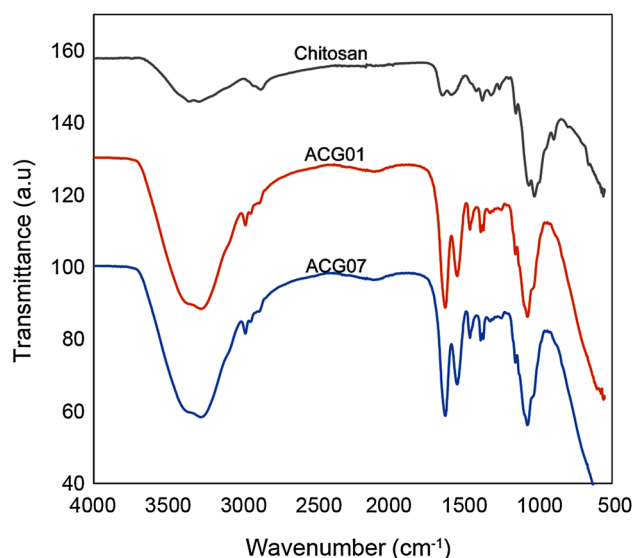


Fig. 1 Typical FTIR spectra of pure chitosan and selected chitosan-PNIPAM microgels

emulsion technique. Detailed microgel compositions with their given code and basic properties are shown in Table 1. The chemical structures of the pure chitosan and chitosan-PNIPAM microgels were confirmed by FTIR spectroscopy. Figure 1 shows the typical FTIR spectra of pure chitosan and some representative microgels.

Different IR peaks at various/specific positions corresponding to different functional groups can be seen in Fig. 1. FTIR spectra of pure chitosan shows a broad band at approximately 3300–3400 cm^{-1} which was assigned to the stretching vibration of hydroxyl groups; this peak overlapped the N–H stretching vibration in the same region. The absorption peaks at 2872 cm^{-1} were associated with the C–H stretching of methylene and methyl groups of glycol chitosan. The characteristic absorption peaks of the chitosan at 1650–1560 cm^{-1} can be assigned to the carbonyl stretching and the stretching vibration of the amino group (amide bands) of the aminoacetyl group of chitosan, whilst that at 1373.5 cm^{-1} is assigned to the vibration of C–H. The peak of 2872.35 cm^{-1} is a typical C–H vibration. Similarly, the peaks at approximately 894.07, 1150.35, and 1560 cm^{-1} , which correspond to the saccharide structure of chitosan, are also present. The broad peak at 1061.71 indicates C–O stretching vibration [34]. Furthermore, the peaks at 1158.60 and 1253 cm^{-1} can be assigned to C–N stretching of the amino group of chitosan.

Compared to that of the pure chitosan, the FTIR profiles of the chitosan-PNIPAM hydrogels were individually monitored. It can be seen that in addition to the appearance of new peaks in the range of 1750–1250 cm^{-1} , the position and intensity of some older peaks is also changed. The peak at 1025.48 cm^{-1} , which indicates C–O stretching

vibration in the spectrum of chitosan, disappeared and the broad peak at 1061.71 cm^{-1} shifted to 1071.85 cm^{-1} in the chitosan-PNIPAM microgel spectra, and became slightly more intense in the microgel sample. The new peaks at $1071\text{--}1155\text{ cm}^{-1}$ can be assigned to the C–N stretching of single bonded chains. The FTIR spectra of chitosan-PNIPAM copolymer hydrogels also show deformation of the two methyl groups on $-\text{C}(\text{CH}_3)_2$ at 1385 and 1362 cm^{-1} , $-\text{CH}_3$ and $-\text{CH}_2$ deformation at 1460 cm^{-1} , $-\text{CH}_3$ symmetric stretching at $2800\text{--}2880\text{ cm}^{-1}$ and $-\text{CH}_3$ asymmetric stretching at 2976 cm^{-1} of the PNIPAM moieties. Two new stronger peaks, corresponding to amide I and II groups of PNIPAM, at 1626 and 1546 cm^{-1} , respectively, also appeared in the hydrogel samples. A minor but broader peak in the range $2000\text{--}2400\text{ cm}^{-1}$ can be assigned to the intermolecular hydrogen bonding and hence the physical crosslinking in the hydrogel. The FTIR spectra of all other microgels, which are not shown here, have almost the same FTIR pattern as those of the presented microgels. Shifting of the positions, shape and intensities of various peaks in the microgels, as compared to pure chitosan, are indications of microgel formation. Further, an increase in the intensity and change in the shape of the $3100\text{--}3500\text{ cm}^{-1}$ absorption band, with changing NIPAM to chitosan ratio in the feed, also supports the incorporation and crosslinking of chitosan in the PNIPAM matrix [35].

Effect of chemical composition on the hydrodynamic size of microgels

Dynamic light scattering was used to investigate the hydrodynamic size of the chitosan-PNIPAM based microgels, in the form of hydrodynamic diameter (D_h) at various temperatures and pHs. During a typical DLS experiment, the intensity auto-correlation functions of the fluctuating signals $G_{(\tau)}^{(2)}$ were measured and analysed using the well-known constrained regularized CONTIN method [36]. Distributions of decay rate, Γ were converted to distributions of apparent mutual diffusion coefficient [37]:

$$D_{\text{app}} = \Gamma/q^2 \quad (1)$$

In Eq. (1), the scattering vector $q = (4\pi n/\lambda) \sin(\theta/2)$, n is the refractive index of the solvent, and θ is the scattering angle. Supposing that the particles are solid, the apparent diffusion coefficient was then converted to an apparent hydrodynamic diameter [$D_{h,\text{app}}$, diameter of the hydrodynamically equivalent hard sphere, corresponding to the apparent diffusion coefficient (D_{app})], using the Stokes–Einstein relationship [38]:

$$D_{h,\text{app}} = kT/(3\pi\eta D_{\text{app}}) \quad (2)$$

where, k is the Boltzmann constant, T is the absolute temperature, and η is the viscosity of the solvent. In actual

practice, intensities $I(\Gamma)$, delivered by the CONTIN program at logarithmically spaced values of decay rate, were transformed to $I(\log\Gamma) = I(\Gamma)\Gamma$ to obtain the intensity distributions of $\log(\Gamma)$, and so $\log(D_{h,\text{app}})$. The normalization of $I(\log D_{h,\text{app}})$ gave intensity fraction distributions. Average values of Γ , delivered by the CONTIN program by integration over the intensity distributions, were similarly converted to intensity-average values of $D_{h,\text{app}}$ [37, 38]. It is important to mention here, that the values of sizes (D_h) given in this paper are the average values; and hence, slightly overestimated, as soft particles possess lower D_h than the real hard sphere ones for frictional reasons. The average size (D_h) of hydrogels at constant temperature ($T = 25\text{ }^\circ\text{C}$) and $\text{pH} \approx 6$ are given in Table 1.

It can be seen from Table 1 that, at constant temperature and pH, the microgel size clearly depends on the chemical/feed composition of the microgel. This behaviour can also be further clarified from D_h -temperature profile (Fig. 3) which is briefly discussed in the next section. On the average, hydrogel size increases with increasing cross-linker (MBA) content in the feed up to 20 mg per 100 mL of reaction mixture while further increase in the cross-linker ratio reduces the microgel size. The first increase in the microgel size with cross-linker can be assigned to the more entrapping of chitosan molecules into the microgel matrix by MBA. In other words, the proportion of chitosan that could be entrapped in the PNIPAM matrix may increase with cross-linker ratio. However, the decrease in the microgel size with MBA ratio, at 30 mg per 100 mL of the reaction mixture, can be due to increase in crosslinking density of the microgel. This may result in the microgel particles with less swollen and tight/compact structure. To eliminate any experimental error and confirm this special trend of the microgel size with cross-linker content, each experiment was repeated many times but the same trend as reported in Table 1 was obtained. In a more comprehensive way, we can say that the increase in the crosslinking agent would increase the conversion and crosslinking density. In addition, the grafting ratio might increase as well. As a result, the particle size would increase when the monomer conversion and grafting ratio were increased, but would decrease when the crosslinking density was increased. The former two factors dominated when the MBA was increased to 20 mg per 100 mL but the latter factor dominated when it was further increased to 30 mg per 100 mL. It can be further seen that the size of the microgel also varies with changing the content of NIPAM in the microgel while keeping the amount of other moieties constant. An increase in the size of microgels can be observed with NIPAM/chitosan ratio ranges from 1 to 2. This situation is understandable as it may increase the incorporation of number of chitosan chains in the microgel and hence will result in higher degree of copolymerization. However, a little reduction

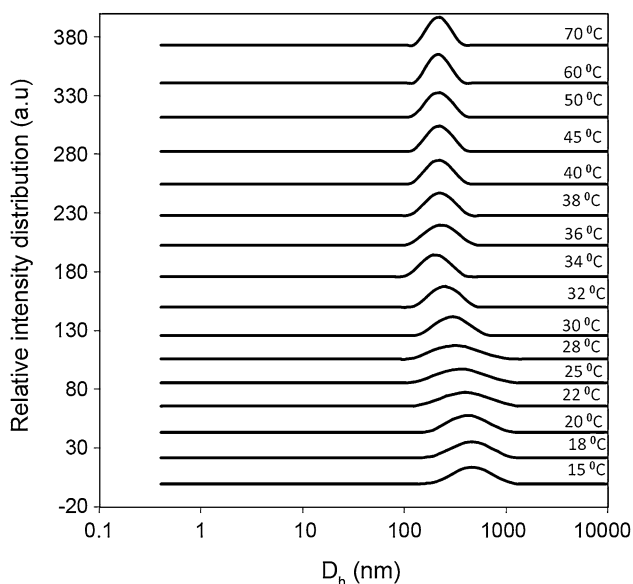


Fig. 2 Plots of intensity distributions of apparent hydrodynamic diameter for aqueous solutions of ACG06 at different temperatures and under pH \approx 6

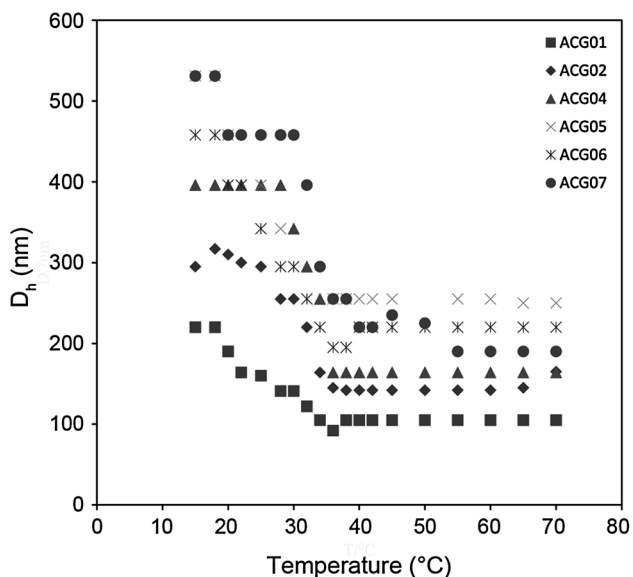


Fig. 3 Dependence of the average hydrodynamic diameter on temperature for different chitosan-PNIPAM microgels in aqueous solutions at pH \approx 6

in the size of hydrogel was seen when the NIPAM/chitosan ratio was further increased to 3. As a result of this phenomenon, the population density or number of hydrogel particles having relatively smaller size may increase instead of increasing the size of individual particle. This is because the higher content of NIPAM can enhance the hydrophilic capacity of the hydrogels which will increase

polymer–solvent interactions as compared to polymer–polymer interactions below its LCST [39]. It is necessary to remind here, that the discussion in this section is at a temperature ($T = 25$ °C) which is below the LCST of PNIPAM. At $T < \text{LCST}$, both chitosan and PNIPAM are hydrophilic in nature, though PNIPAM is expecting to be more hydrophilic compared to chitosan because of its chemical nature. Therefore, on the average, variation of hydrogel size due to changing the NIPAM/chitosan ratio and amount of cross-linker can be assigned to the change in hydrophilic–hydrophobic balance of hydrogels.

Temperature-induced volume phase transitional behaviour of the hydrogels

To explore the potential application of stimuli-responsive smart microgels, it is very important to investigate the effect of temperature on their volume phase transitional changes [6, 39]. For this reason we studied the effect of temperature on the physicochemical properties of chitosan-PNIPAM based microgel/hydrogels in an aqueous medium. Figure 2 shows the typical intensity fraction distributions of apparent D_h plots from DLS at various temperatures ranging from 15 to 70 °C for ACG06 in water while keeping the pH of the medium constant pH (pH \approx 6). Average values of D_h were obtained from the maxima of each peak of such distribution plots. It was observed that the shapes and positions of these peaks shifted along with the changing temperature of the microgel solutions. To see the effect of temperature and chemical composition on the hydrodynamic size and volume phase transition temperature (VPTT), we have plotted the values D_h for each microgel as a function of temperature in Fig. 3. On an overview, D_h decreases with increasing temperature, indicating the shrinking of the microgels. However, it is significant to mention that the reduction of the size with temperature for all hydrogel samples reaches a plateau somewhat once the temperature becomes close to or higher than the LCST of PNIPAM. Moreover, this deflection point in the D_h -temperature profile varies with changing the composition of microgels. In case of chitosan-PNIPAM polymeric hydrogels, there exists a fine hydrophobic–hydrophilic balance in their chemical structure. Thus, based on D_h -temperature profile outcomes, the thermo-sensitive behaviour of the microgels under study can be attributed to the alternation in hydrophilicity/hydrophobicity balance of the network. It is because for stimuli-responsive polymers, the polymer–polymer and the polymer–solvent interactions can show an unexpected re-adjustment in small/specific ranges of pH or temperature changes, and this is translated into a chain transition between extended and compacted coil states [29]. Therefore, some changes in the solution temperature, around the critical temperature, make the chains to collapse or to

expand responding to the new adjustments of the hydrophobic and hydrophilic interactions between the polymeric chains themselves and with the water. The earlier studies of PNIPAM homopolymer chains revealed that when the solution temperature is lower than the lower critical solution temperature (LCST ≈ 32 °C), PNIPAM is hydrophilic and exists as individual random coil chains in water, while at higher temperatures ($T > \text{LCST}$), PNIPAM becomes hydrophobic and collapses depending on the overall condition of solution [40].

Furthermore, we were expecting that the hydrophilic chitosan moieties will not only affect the hydrodynamic size of microgels but should also have significant impact on the VPTT of our chitosan-PNIPAM based microgels. The effect of chemical composition and various contents in the feed on the D_h is already discussed in the previous section. Figure 3 shows that VPTT changes by varying the ratio of NIPAM/chitosan and also by the amount of cross-linker (MBA) in the reaction feed. This effect can be assigned to the variation of hydrophilic-hydrophobic balance due to alteration of the incorporation of number chitosan chains in the microgel while changing NIPAM/chitosan ratio. This is important to note that at $T > \text{LCST}$, PNIPAM becomes hydrophobic and collapses, while chitosan is still hydrophilic and affects the VPTT range of microgels. At $T > 40$ °C, there is no prominent change in the size of microgels with further increasing temperature; this effect may arise due to the presence of chitosan, which contains rigid polysaccharide chains and thereby hinders further contraction of hydrogel particles. Similarly, varying the amount of cross-linker in the hydrogels may not only change the physicochemical combination of chitosan with the PNIPAM matrix but also results in hydrogel particles with different swelling ratios. It can also be said that chitosan-PNIPAM hydrogels having different swelling ratios may have dissimilar particle structure/morphology and hence different LCST/VPTT. The previous studies of PNIPAM based copolymer also showed that LCST depends on the morphology of copolymer particles [33]. As supposed here, hydrogel particle having different structures may have different degrees of polymer–polymer and polymer–solvent interactions which can affect their corresponding LCST/VPTT values in aqueous media. It is worth mentioning that the change of temperature-induced On/Off (swelling/deswelling) window for chitosan-PNIPAM based hydrogels by varying the chemical composition of the microgels is important from biomedical point of view. On an overview, it can be seen from Fig. 3 that, almost for all microgel samples tested, complete de-swelling/shrinkage occurs in the temperature range 36–39 °C. As this temperature range is near to human body temperature, hence it reflects the applications of these hydrogels as potential drug delivery system.

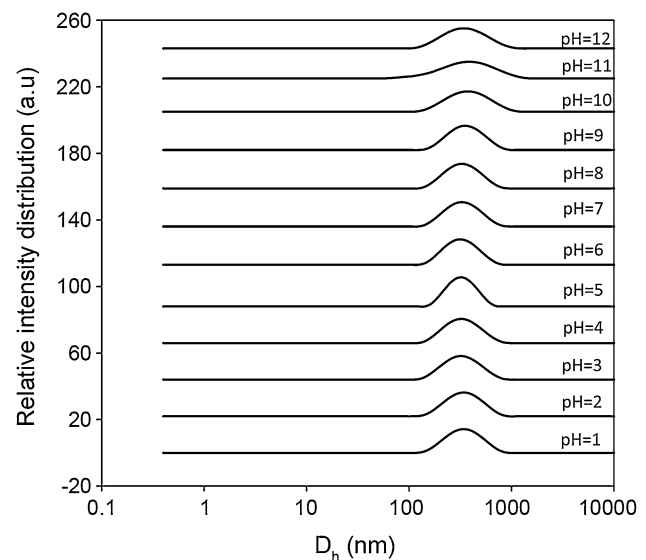


Fig. 4 Plots of intensity distributions of apparent hydrodynamic diameter for aqueous solutions of ACG06 at different pH and $T = 25$ °C

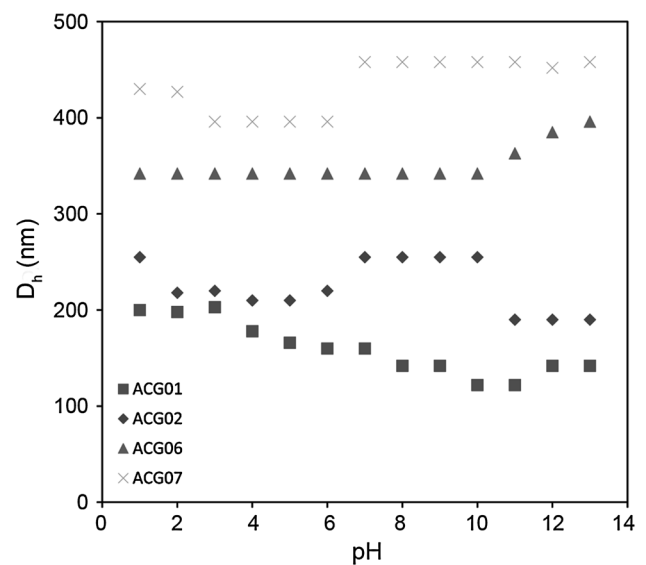


Fig. 5 Plots of average hydrodynamic diameter as a function of pH for different chitosan-PNIPAM microgels in aqueous solutions at $T = 25$ °C

Effect of pH on volume phase changes and stability of chitosan-PNIPAM microgels

To better understand the physicochemical properties, stability and especially the “On/Off” behaviour of the synthesized chitosan-PNIPAM hydrogels in aqueous media, we also investigated the effect of pH on microgel size (D_h) at room temperature. As chitosan is known as a pH-sensitive biomaterial and its hydrophilic character varies

with change in pH of the medium [21]. However, PNIPAM moiety of our hydrogel system is not a typical pH-sensitive polymer. The typical intensity fraction distributions of the apparent hydrodynamic diameter plots from DLS at various pHs and 25 °C for ACG06 in water are shown in Fig. 4. Meanwhile, the dependence of D_h on pH for four representative microgels is presented in Fig. 5. To see the effect of pH on the microgel size (D_h), we selected four different compositions; one series (ACG06 and ACG07) composed of microgels having the same cross-linker content but different NIPAM/chitosan ratios. Whereas, the second series (ACG01 and ACG02) have similar NIPAM/chitosan ratio but different cross-linker (MBA) contents. It can be seen that, on the average, there is no prominent change in the D_h versus pH profile up to $\text{pH} \approx 6$. However, by further increasing the pH of the investigation medium, different behaviours of pH-dependence of D_h can be observed for microgels having different chemical compositions. The trend of D_h with pH of the solution, as shown in Fig. 5, indicates that chitosan-PNIPAM hydrogels are more stable in acidic and neutral media but less so in basic medium. It is understandable because the pK_a value for chitosan is approximately equal to 6.5, due to which pH-sensitive behaviour, in terms of D_h , varies with pH of hydrogel solution [41]. The less prominent change in D_h -pH profile, and hence the stability in acidic and neutral pH regions, can be attributed to the presence of positive charges on the surface of hydrogel particles. These charges arise due to the protonation of amino ($-\text{NH}_2$) groups of chitosan to a positively charged ($-\text{NH}_3^+$) groups when $\text{pH} < \text{pK}_a$ of chitosan. This makes the hydrogels friendlier to aqueous media due to increased hydrophilicity. However, in the neutral pH region, the amino groups are not or much less protonated, so the stability can be attributed to the presence of hydrophilic PNIPAM. The change in microgel size in the alkaline pH region may arise due to inter-particle interactions. Because some of the hydroxyl groups of chitosan can be ionized/deprotonated. Further information and clarification can be found from the behaviour of zeta potential with pH in the next section.

Moreover, it is important to mention here that although the true solubility of pure chitosan chain is limited only to acidic media, but chitosan-PNIPAM particles remained soluble and maintained their stability in water in a wide range of pH ($\text{pH} \approx 2$ –8) for about 3 months at room temperature. This significant outcome, of our general/naked-eye observations, indicates that chitosan chains are not only attached physicochemically to PNIPAM but also have chemical linkage with PNIPAM networks. Thus, it can be said that the chitosan-PNIPAM hydrogels, reported in this work, resulted in improved particles with better stability in acid, neutral, and alkaline aqueous solution, as compared to unmodified PNIPAM and chitosan only. Furthermore,

the degree of stability also depends on the chemical composition, for example the ratio of NIPAM/chitosan and the amount of cross-linker (MBA) in the feed composition. After 3 months, the hydrogels having lower NIPAM/chitosan exhibited some sedimentation/aggregation at or above $\text{pH} \approx 8$ of the medium. This effect can be attributed to the decrease in hydrophilic capacity with decrease in NIPAM content.

Effect of pH on the electrophoretic mobility of microgel particles

The stability, swelling/de-swelling, and physicochemical information under different pH conditions can be obtained by knowing the electrical state of ionisable groups of the chitosan-PNIPAM microgel particles. For this reason the electrophoretic mobility (μ) and zeta potential (ζ) were measured as a function of pH of the medium for four representative microgels having different compositions. The reported values of ζ -potential were calculated from the electrophoretic mobilities (μ) of hydrogel particles using the relationship [29]:

$$\zeta = \frac{3\mu\epsilon_0}{2\epsilon_0\epsilon_r \times f(ka)} \quad (3)$$

Here, ϵ_0 is the permittivity of vacuum, ϵ_r is the relative permittivity of the medium, and η is the viscosity of water. The values of ϵ_0 , ϵ_r , and η were taken as $8.854 \times 10^{-4} \text{ J}^{-1} \text{ C}^2 \text{ m}^{-1}$, 78.5, and $8.904 \times 10^{-4} \text{ Nm}^{-2} \text{ s}$, respectively. Similarly, the factor $f(ka)$, known as the Henry factor, depends on particle shape; for a sphere with $ka > 1$ it is given by [30]:

$$f(ka) = \frac{3}{2} + \frac{9}{2ka} + \frac{75}{2k^2a^2} - \frac{330}{k^3a^3} \quad (4)$$

In Eq. (4), k is the reciprocal of Debye length. For the present case, the product ka was approximately 2.1, which corresponds to $f(ka) \approx 1.04$. The behaviour of zeta potential as a function of pH of the medium, for four compositions tested, is shown in Fig. 6.

As seen, for all microgels, the zeta potential changes along with the changing pH of the medium, indicate their pH-sensitivity due to the presence of chitosan moieties. It can be seen that the zeta potential values are positive for all microgels in the acidic pH region ($\text{pH} \approx 1.4$ –6). On the average, these values decrease with an increasing pH of the medium until reaching neutral pH ($\text{pH} \approx 6.3$ –7.5). The positive values of zeta potential at $\text{pH} < \text{pK}_a$ (6.5) of chitosan, are assigned to the presence of positive charges on the surface of hydrogel particles arise due to protonation of amino ($-\text{NH}_2$) groups of chitosan to positively charged ($-\text{NH}_3^+$) groups. Further, in neutral pH region, the values of zeta potential become almost equal to zero, which

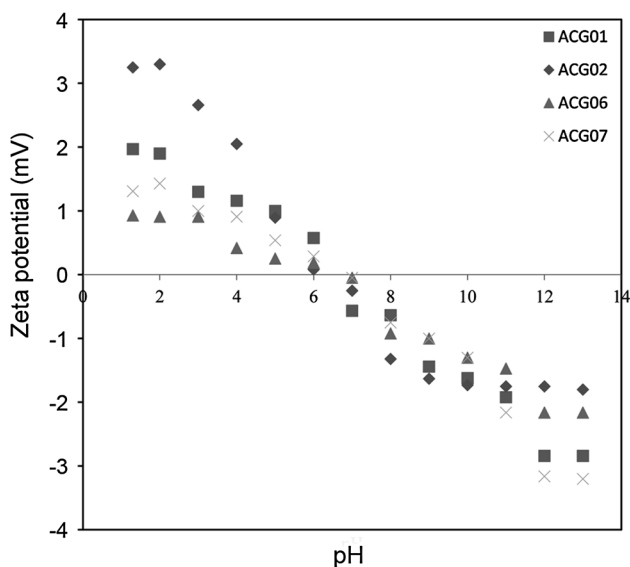


Fig. 6 Dependence of zeta potential on the pH of the medium for aqueous solutions of different chitosan-PNIPAM microgels at $T = 25\text{ }^{\circ}\text{C}$

reflects that the amino groups of chitosan are no more or much less protonated. Thus, this region in the zeta potential-pH profile can be assigned as the isoelectric point of the hydrogels, at which the microgel particles are expected to be uncharged. Moreover, Fig. 5 also reveals that in alkaline pH region ($\text{pH} > 7.5$) hydrogels exhibit negative zeta potential values which become more negative with increasing pH of solution. This situation arises due to ionization/de-protonation of some of the hydroxyl ($-\text{OH}$) groups of chitosan and also due to some contribution of the anionic nature of the initiator (APS) used in this study. There is no prominent change in zeta potential when $\text{pH} > 11$, meaning that ionization capacity of hydroxyl ($-\text{OH}$) groups has already reached to its maximum limit. It is worth mentioning that irrespective of the sign (either +ve or -ve), the zeta potential values are less than four which suggest the stability of microgels over a wide range of pH at constant temperature. The effect of microgel composition on the behaviour of zeta potential, at $\text{pH} \approx 6$ and $T = 25\text{ }^{\circ}\text{C}$, can be seen in Table 1. Again the zeta potential values, for all samples, are very close to zero reflecting the uncharged or partially charged state of hydrogels at $\text{pH} \approx 6$. The slight change in zeta potential, for the microgels having different chemical compositions, can be attributed to the variation of hydrophilic-hydrophobic balance which indirectly affects the interaction with solvent and hence the charge density on the particles. Finally, in addition to the quality/quantity of microgel charge, zeta potential results also support the stability and swelling/de-swelling behaviour of microgel in response to the pH of its environment.

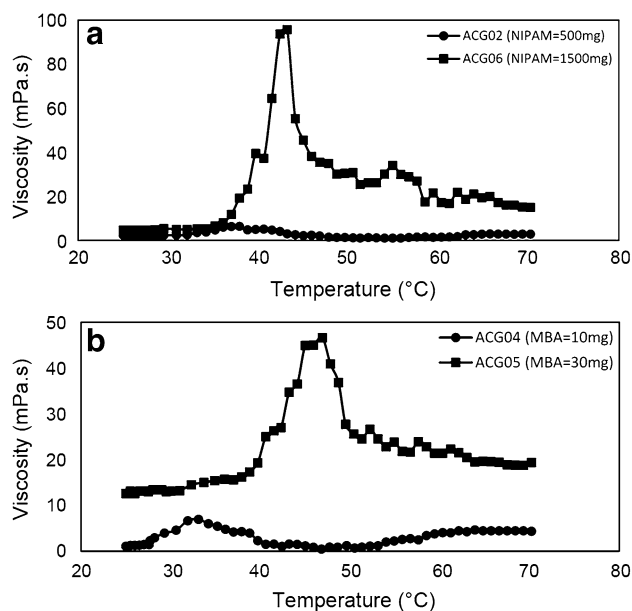


Fig. 7 Apparent viscosity as a function of temperature for chitosan-PNIPAM microgels at constant shear rate and $\text{pH} \approx 6$, **a** different NIPAM contents and **b** different cross-linker amount

Effect of temperature and chemical composition on the rheological behaviour of hydrogels

The rheological studies of stimuli-responsive polymers in aqueous media, is very helpful to elucidate the phase changes and association behaviour in response to shear rate applied at different pH and temperatures [42, 43]. The temperature-dependence of chitosan-PNIPAM hydrogel viscosity, in aqueous media at a constant $\text{pH} \approx 6$, is shown in Fig. 7. It can be seen that, for the four selected hydrogels, there is no prominent change in viscosity with temperature up to 28–29 $^{\circ}\text{C}$. However, at temperatures beyond these, the viscosity increases slowly and after reaching a certain temperature, which can be called as VPTT, an abrupt increase in viscosity is observed. The drastic increase in viscosity at/above VPTT can be assigned to the appearance of gelation/association process [44]. Moreover, after reaching a peak point, the viscosity starts to decrease with further increase in temperature. This may occur due to dehydration and shear thinning effects. At $T > 50\text{ }^{\circ}\text{C}$, fewer changes in viscosity-temperature profile can be seen. Previously, it was observed that when swollen particles are subjected to a temperature above LCST of PNIPAM, the particles shrink. The phenomenon happens as a result of disruption of hydrogen bonding with water molecules and the formation of hydrophobic associations among isopropyl moieties of PNIPAM [45, 46]. Consequently, a resistance to flow and hence increase in viscosity at low shear rates can be observed due to formation of compact particles [47].

However, further increase in temperature (above 50 °C) may cause dehydration of hydrogels and hence weaken the association of collapsed particles which leads to decrease in viscosity due to an indirect shear thinning effect. It is important to mention here that de-swelling/shrinkage of the hydrogels particle with temperature beyond VPTT was also observed in our dynamic light scattering results (Fig. 3). The appearance of gelation behaviour, at/above VPTT, in response to temperature was also observed through visual analysis of tube inversion method. At this point we also wish to stress that temperature can disrupt/disturb both intra- and inter-polymer association, but with opposite effects.

Moreover, it can also be seen from Fig. 7a, b that chemical composition of chitosan-PNIPAM based hydrogels greatly affects their rheological behaviour. Both of these figures clarify that varying the chemical composition, such as NIPAM/chitosan ratio and cross-linker (MBA) contents of the chitosan-PNIPAM hydrogel systems, not only affect the values of viscosity but also alter the VPTT. Figure 7a shows that the values of both viscosity and VPTT are higher for hydrogels with greater NIPAM/chitosan ratio. It is because that hydrogels having more PNIPAM may not only enhance the hydrophilicity of hydrogels but also increase the incorporation of number chitosan chains in the microgel. Similarly, Fig. 7b shows that the average viscosity and VPTT increase with increasing the cross-linker (MBA) content in the feed. As microgels with higher cross-linker content may result in particles with less swollen/compact structure, which may exhibit more resistance to flow and hence increase in viscosity of the system. Moreover, the proportion of chitosan that could be entrapped in the PNIPAM matrix may also increase with cross-linker ratio. Importantly, from biomedical point of view ideal injectable hydrogels should offer low resistance to shear flow so that hydrogel can easily flow with less consumption of energy. Otherwise, they should not be suitable for biomedical applications. It can be easily realised from our viscosity results that, on the average, the hydrogels under present investigation exhibit low viscosity and can be used for potential biomedical applications.

Conclusions

The soapless emulsion free-radical copolymerization method was successfully employed to prepare six different compositions of dual-responsive chitosan-PNIPAM copolymer microgels. The swelling/de-swelling, volume phase transitions, electrical properties, colloidal stability, and rheological behaviour of different compositions of chitosan-PNIPAM microgels have been investigated in aqueous medium under various conditions of temperature

and pH for their potential applications. DLS results show that the size (D_h) of the particle decreases with increasing temperature up to 38 °C, indicating the shrinkage of the microgels. Moreover, the size and VPTT are affected by varying the chemical composition of the microgels, this effect can be assigned to the alternation in hydrophilicity/hydrophobicity balance of the network. Further, the complete de-swelling/shrinkage occurs in the temperature range 36–39 °C, and as this temperature range is near to human body temperature, hence it reflects the applications of these hydrogels as potential drug delivery system. The size of microgels was found to be quite stable at $T > 40$ °C and pH 6. Though, a transition from sol-to-gel behaviour with temperature beyond 50 °C was also noticed through visual observation. It was also observed that most of chitosan-PNIPAM particles remained soluble and maintained good stability without significant sedimentation in water through a wide range of pH (pH \approx 2–8) for about 3 months at room temperature. This indicates that the chitosan chains are not only attached physicochemically to PNIPAM but also have chemical linkage with PNIPAM networks. Irrespective of the sign (either +ve or –ve), zeta potential values are less than four, which further reflects that these chitosan-PNIPAM hydrogels resulted in improved particles with better stability in acid, neutral, and alkaline aqueous solution, as compared to unmodified PNIPAM and chitosan only. The temperature-induced sol–gel behaviour and volume phase changes of the hydrogels were further confirmed by rheological studies. After detailed physicochemical investigations, we conclude that most of the properties of hydrogel such as swelling/de-swelling, volume phase transitions, electrical properties, colloidal stability, and rheological behaviour are not only influenced by changing the chemical compositions of microgels but also by varying the pH/temperatures of the medium. Finally, the present study suggests that these dual-responsive microgels with adjustable properties promise important applications in the fields of biomedical and biotechnology.

Acknowledgments Dr. Abbas Khan is extremely grateful to the Academy of Sciences for developing countries (TWAS) and USM for TWAS-USM Post-Doctoral research fellowship. He also wishes to acknowledge Abdul Wali Khan University Mardan Pakistan for postdoc study leave. The authors also wish to thank the Ministry of Science, Technology and Innovation (MOSTI) Malaysia for sponsoring the project under the Fundamental Research Grant Scheme FRGS/203/PBAHAN/6071242.

References

1. Murthy N, Xu M, Schuck S, Kunisawa J, Shastri N, Fréchet JM (2003) A macromolecular delivery vehicle for protein-based vaccines: acid-degradable protein-loaded microgels. *Proc Natl Acad Sci* 100:4995–5000

2. Morris GE, Vincent B, Snowden MJ (1997) Adsorption of lead ions onto *N*-isopropylacrylamide and acrylic acid copolymer microgels. *J Colloid Interface Sci* 190:198–205
3. Sun HQ, Zhang L, Li ZQ, Zhang L, Luo L, Zhao S (2011) Interfacial dilational rheology related to enhance oil recovery. *Soft Matter* 7:7601–7611
4. Retama JR, Lopez-Ruiz B, Lopez-Cabarcos E (2003) Microstructural modifications induced by the entrapped glucose oxidase in cross-linked polyacrylamide microgels used as glucose sensors. *Biomaterials* 24:2965–2973
5. Bagheri M, Shateri Sh (2012) Thermosensitive nanosized micelles from cholesteryl-modified hydroxypropyl cellulose as a novel carrier of hydrophobic drugs. *Iran Polym J* 21:365–373
6. Farooqi ZH, Khan A, Siddiq M (2011) Temperature-induced volume change and glucose sensitivity of poly [(*N*-isopropylacrylamide)-co-acrylamide-co-(phenylboronic acid)] microgels. *Polym Int* 60:1481–1486
7. Zhang J, Xu S, Kumacheva E (2004) Polymer microgels: reactors for semiconductor, metal, and magnetic nanoparticles. *J Am Chem Soc* 126:7908–7914
8. Nilsson P, Hansson P (2005) Ion-exchange controls the kinetics of deswelling of polyelectrolyte microgels in solutions of oppositely charged surfactant. *J Phys Chem B* 109:23843–23856
9. Nisato G, Munch JP, Candau SJ (1999) Swelling, structure, and elasticity of polyampholyte hydrogels. *Langmuir* 15:4236–4244
10. Dowding PJ, Vincent B, Williams E (2000) Preparation and swelling properties of poly (NIPAM) minigel particles prepared by inverse suspension polymerization. *J Colloid Interface Sci* 221:268–272
11. López-León T, Elaïssari A, Ortega-Vinuesa JL, Bastos-González D (2007) Hofmeister effects on poly (NIPAM) microgel particles: macroscopic evidence of ion adsorption and changes in water structure. *Chem Phys Chem* 8:148–156
12. Freiberg S, Zhu XX (2004) Polymer microspheres for controlled drug release. *Int J Pharm* 282:1–18
13. Gautrot JE, Zhu XX (2006) Biodegradable polymers based on bile acids and potential biomedical applications. *J Biomater Sci-Polym Ed* 17:1123–1139
14. Oh JK, Lee DI, Park JM (2009) Biopolymer-based microgels/nanogels for drug delivery applications. *Prog Polym Sci* 34:1261–1282
15. Bhattarai N, Gunn J, Zhang M (2010) Chitosan-based hydrogels for controlled, localized drug delivery. *Adv Drug Deliv Rev* 62:83–99
16. Mao S, Sun W, Kissel T (2010) Chitosan-based formulations for delivery of DNA and siRNA. *Adv Drug Delivery Rev* 62:12–27
17. Zhang L, Gu F, Chan J, Wang A, Langer R, Farokhzad O (2007) Nanoparticles in medicine: therapeutic applications and developments. *Clin Pharmacol Ther* 83:761–769
18. Muzzarelli RA, Morganti P, Morganti G, Palombo P, Palombo M, Biagini G, Mattioli Belmonte M, Giantomassi F, Orlandi F, Muzzarelli C (2007) Chitin nanofibrils/chitosan glycolate composites as wound medicaments. *Carbohydr Polym* 70:274–284
19. Tan H, Marra KG (2010) Injectable, biodegradable hydrogels for tissue engineering applications. *Materials* 3:1746–1767
20. Sonia TA, Sharma CP (2011) Chitosan and its derivatives for drug delivery perspective. In: Jayakumar R, Prabaharan M, Muzzarelli RAA (eds) *Chitosan for biomaterials I*. Springer, Heidelberg, pp 23–53
21. Zhang H, Mardiyani S, Chan WCW, Kumacheva E (2006) Design of biocompatible chitosan microgels for targeted pH-mediated intracellular release of cancer therapeutics. *Biomacromolecules* 7:1568–1572
22. López-León T, Carvalho EL, Seijo B, Ortega-Vinuesa JL, Bastos-González D (2005) Physicochemical characterization of chitosan nanoparticles: electrokinetic and stability behavior. *J Colloid Interface Sci* 283:344–351
23. Khalid MN, Agnely F, Yagoubi N, Grossiord JL, Couarraze G (2002) Water state characterization, swelling behavior, thermal and mechanical properties of chitosan based networks. *Eur J Pharm Sci* 15:425–432
24. Shin MS, Kim SI, Kim IY, Kim NG, Song CG, Kim SJ (2002) Characterization of hydrogels based on chitosan and copolymer of poly (dimethylsiloxane) and poly (vinyl alcohol). *J Appl Polym Sci* 84:2591–2596
25. Tian XX, Groves MJ (1999) Formulation and biological activity of antineoplastic proteoglycans derived from *Mycobacterium vaccae* in chitosan nanoparticles. *J Pharm Pharmacol* 51:151–157
26. Banerjee T, Mitra S, Kumar Singh A, Kumar Sharma R, Maitra A (2002) Preparation, characterization and biodistribution of ultrafine chitosan nanoparticles. *Int J Pharm* 243:93–105
27. Schatz C, Pichot C, Delair T, Viton C, Domard A (2003) Static light scattering studies on chitosan solutions: from macromolecular chains to colloidal dispersions. *Langmuir* 19:9896–9903
28. Imran AB, Seki T, Takeoka Y (2010) Recent advances in hydrogels in terms of fast stimuli responsiveness and superior mechanical performance. *Polym J* 42:839–851
29. Haraguchi K, Li HJ (2005) Control of the coil-to-globule transition and ultrahigh mechanical properties of PNIPA in nanocomposite hydrogels. *Angew Chem Int Ed* 44:6500–6504
30. Jones CD, Lyon LA (2000) Synthesis and characterization of multiresponsive core-shell microgels. *Macromolecules* 33:8301–8306
31. Schild HG (1992) Poly (*N*-isopropylacrylamide): experiment, theory and application. *Prog Polym Sci* 17:163–249
32. Prabaharan M, Mano JF (2006) Stimuli-responsive hydrogels based on polysaccharides incorporated with thermo-responsive polymers as novel biomaterials. *Macromol Biosci* 6:991–1008
33. Lee CF, Wen CJ, Lin CL, Chiu WY (2004) Morphology and temperature responsiveness–swelling relationship of poly (*N*-isopropylamide–chitosan) copolymers and their application to drug release. *J Polym Sci Part A: Polym Chem* 42:3029–3037
34. Krishna Rao KSV, Vijaya Kumar Naidu B, Subha MCS, Sairam M, Aminabhavi TM (2006) Novel chitosan-based pH-sensitive interpenetrating network microgels for the controlled release of cefadroxil. *Carbohydr Polym* 66:333–344
35. Verestuec L, Ivanov C, Barbu E, Tsibouklis J (2004) Dual-stimuli-responsive hydrogels based on poly(*N*-isopropylacrylamide)/chitosan semi-interpenetrating networks. *Int J Pharm* 269:185–194
36. Provencher SW (1979) Inverse problems in polymer characterization: direct analysis of polydispersity with photon correlation spectroscopy. *Makromol Chem* 180:201–209
37. Khan A, Siddiq M (2013) Light scattering and surface tensiometric studies of tip-modified PEO–PBO diblock copolymers in water. *J Polym Res* 20:1–9
38. Khan A, Farooqi ZH, Siddiq M (2012) Associative properties of hydrophilic tip modified oxyethylene-oxybutylene diblock copolymers in aqueous media: effect of end-group. *J Appl Polym Sci* 124:951–957
39. Wang M, Fang Y, Hu D (2001) Preparation and properties of chitosan-poly(*N*-isopropylacrylamide) full-IPN hydrogels. *React Funct Polym* 48:215–221
40. Wu C, Zhou S (1995) Thermodynamically stable globule state of a single poly(*N*-isopropylacrylamide) chain in water. *Macromolecules* 28:5388–5390
41. Wu W, Shen J, Banerjee P, Zhou S (2010) Chitosan-based responsive hybrid nanogels for integration of optical pH-sensing, tumor cell imaging and controlled drug delivery. *Biomaterials* 31:8371–8381



42. Hietala S, Nuopponen M, Kalliomäki K, Tenhu H (2008) Thermoassociating poly (*N*-isopropylacrylamide) A–B–A stereo block copolymers. *Macromolecules* 41:2627–2631
43. Dumitriu RP, Mitchell GR, Vasile C (2011) Rheological and thermal behaviour of poly (*N*-isopropylacrylamide)/alginate smart polymeric networks. *Polym Int* 60:1398–1407
44. Chen JP, Cheng TH (2009) Preparation and evaluation of thermo-reversible copolymer hydrogels containing chitosan and hyaluronic acid as injectable cell carriers. *Polymer* 50:107–116
45. Spizzirri UG, Iemma F, Puoci F, Xue F, Gao W, Cirillo G, Curcio M, Parisi OI, Picci N (2011) Synthesis of hydrophilic microspheres with LCST close to body temperature for controlled dual-sensitive drug release. *Polym Adv Technol* 22:1705–1712
46. Nolan CM, Gelbaum LT, Lyon LA (2006) ¹H NMR investigation of thermally triggered insulin release from poly (*N*-isopropylacrylamide) microgels. *Biomacromolecules* 7:2918–2922
47. Malkin AY, Semakov AV, Kulichikhin VG (2010) Self-organization in the flow of complex fluids (colloid and polymer systems)—part 1: experimental evidence. *Adv Colloid Interfac Sci* 157:75–90